A Universal Multifractals perspective into the link between rainfall ~~extremes and~~ variability ~~,~~ and temperature

Auguste Gires[1] and Yann Torres[1,2]

[1]HM&Co, École nationale des ponts et chaussées, Institut Polytechnique de Paris, Champs-sur-Marne, France
[2]Military Institute of Engineering (IME), Rio de Janeiro, Brazil

Correspondence: Auguste Gires (auguste.gires@enpc.fr)

Abstract.

The link between rainfall extremes, usually defined as a given percentile or for a given return period, and temperature has been widely investigated using measurement data and / or climate model outputs and notably convection permitting model outputs. A focus was notably on whether findings are consistent with Clausius-Clapeyron relation. ~~A scale dependence of the rate of increase with temperature is commonly reported.~~

Here we investigate ~~how rainfall extremes and more generally~~ more generally how rainfall variability across scales change with temperature, relying on the scale invariant framework of the Universal Multifractals. Extremes, which can be derived from multifractal features are embedded in the study. Rainfall and temperature data from three high resolution measurement campaigns that took place in Northern France between 2018 and 2025 are used. Scaling behaviour is confirmed on two distinct ranges of scales, first at event scale (30 s - 1 h) and then up to synoptic scale (roughly 11 days). Then we find that across both ranges of scales, the scale invariant maximum observable singularity increases on average with greater temperature, which provides a framework to interpret previously ~~observed trends~~ commonly reported trends of a scale dependence of the rate of increase of extremes with temperature.

1 Introduction

Precipitation extremes in general are expected to increase under climate change (Masson-Delmotte et al., 2021). These extremes, at sub-hourly scale, daily scale or larger scale have strong influence on river flooding, storm water management, local (including urban) flooding, debris flows, erosion etc. (e.g., Borga et al., 2014; Fowler et al., 2021), and can trigger in some cases natural disasters.

The main process mentioned in the literature to explain why sub-daily to daily rainfall extremes increase with temperature is thermodynamic Clausius-Clapeyron (CC) relation which quantifies the ability of warmer air to hold more moisture. It is often referred to as CC scaling, but we will not use this formulation here to avoid confusion with the scaling of rainfall ~~fields~~ processes which we will discuss later. More precisely, it states that on average, air can hold roughly 7% more moisture per ^oC. ~~Actually, this rate decreases~~ This rate tends to decrease with increasing temperature. It is ~~of 7.3 %$^oC^{-1}$ at 0 ^oC, 6.4 %$^oC^{-1}$ at 15 ^oC and 6 %$^oC^{-1}$ at 25 ^oC (Panthou et al., 2014). It is~~ often assumed that rainfall extremes should increase at the rate suggested by CC relation. Such statement relies on three assumptions: (i) relative humidity stays roughly the same in future climate conditions, (ii) heavy rainfall events are primarily influenced by the atmospheric water content, and (iii) atmospheric circulation patterns do not undergo significant changes in the future climate (Panthou et al., 2014). Another underlying assumption is that surface temperatures are a good indicator of total precipitable water in a column of air. Depending on the type of rainfall extremes, this may or may not be the case. It is likely to not be the case at time scales greater than a day for which atmospheric dynamics and large-scale circulations play a more dominating role than temperature.

Numerous papers, using data or convection permitting model outputs or a combination of both, have studied the influence of temperature on rainfall extremes (usually quantified with the help of percentiles, typically 90, 95 or 99th; or return period) and how well CC relation is retrieved ~~. For example, Moustakis et al. (2020) used a combination of data and convection permitting model to show that CC expected rate held over most part of mid and high latitudes while deviations were found in the tropics. In a later analysis, centered on US, Moustakis et al. (2021) showed that for a studied duration of one hour, a 20 year return rainfall event became a 7 year one over roughly 75% of grid points.~~

~~In an earlier work, Lenderink and van Meijgaard (2008) explained that climate models outputs seemed consistent with the CC relation, while using data from Netherlands they showed some differences according to studied time scales. For example, they found that the increase of hourly extremes (higher quantiles) with temperature went twice as strong as than expected with CC relations when daily mean temperature exceeds 12~~ ~~^oC~~~~. This was further confirmed in a more recent study over the Netherlands and related to the physics of convective clouds (Lenderink et al., 2017). Results from Lenderink and van Meijgaard (2008) were challenged by Haerter and Berg (2009) who considered them as not physical and a statistical artifact. According to their interpretation, it stemed from the combination of stratiform and convective rainfall regimes, both exhibiting CC behaviour but with differing strengths. As temperaturerises and the stratiform-to-convective ratio declines, the effective sealing can reach approximately two CC over a restricted temperature interval.~~

~~Haerter et al. (2010) used 30 years of 5 min data from six stations in Germany and showed that CC relation does not provide a good explanation at all scales. Indeed, they found a stronger increase of extremes with temperature at shorter scales and reported continuous changes.~~

~~Drobinski et al. (2016) studied simulations and measurements collected on Southern France and reported that precipitation extremes increased at rates close to CC relationship at a low temperature regime (below around 15~~ ~~^oC~~~~), while they changed to sub CC rates and even often decreased at high temperature (above around 15~~ ~~^oC~~depending on the temporal scale, temperature range and location Lenderink and van Meijgaard (2008); Haerter and Berg (2009); Haerter et al. (2010); Panthou et al. (2014); Drobinski e . A key observation is that there seems to be a strong scale dependence on the increase of rainfall extremes with temperature, i.e. the increase seems stronger, and stronger than expected from CC relation only, for short durations (typically sub-hourly).

~~Chen et al. (2021) studied data from Eastern China, and also found more pronounced increase of rainfall extremes than expected with CC relation . The wettest 10 hours increased twice faster than CC, while the 10 heaviest daily rainfalls increased three time faster.~~

~~Changes not onlywith temporal scale, but also with region were found. For example Panthou et al. (2014) studied rainfall data, and more precisely the 90 and 99th percentiles, with time steps ranging from 5 min to 12 h for more than 100 meteorological~~

~~stations across Canada. They also found that with longer durations, the increase of extreme rainfall with temperature was less pronounced. They reported differences according to regions. For example, CC relation holds for coastal regions and short durations , while it is not the case for inland regions where super CC is observed, before an upper limit is reached.~~

~~A dependence on temperature is also observed. For example, Sharma and Mujumdar (2019) used datafrom India and observed at daily scale deviations from CC relation, with stronger increase of extremes between~~ ~~25^oC~~ ~~to~~ ~~30^oC~~~~, and less for greater temperature.~~

Similar dependence on spatial scale is also reported by Peleg et al. (2018) who studied high resolution radar data. Precipitations patterns are complex as they arise from the interplay between various non-linear processes. It leads to increases or decreases with regard to thermodynamic relation alone, i.e. CC relation. Such changes in local atmospheric dynamics explain deviations from CC relations. ~~As discussed above, it appears that such deviations depend on temporal scale, with shorter durations rainfall exhibiting an increase rate stronger than expected (Fowler et al., 2021). Similar dependence on spatial scale is also reported by Peleg et al. (2018) who studied high resolution radar data.~~

In order to quantify the impact of climate change on rainfall extremes, some authors used another approach. They relied on a model for extreme value and studied the dependence of key parameters on temperature. For example, Marra et al. (2024) fitted, on data from Switzerland, a non-asymptotic statistical model for extreme rainfall whose parameters depended on temperature. Moustakis et al. (2021) found an increase in tail heaviness of rainfall, and related this to changes in characteristic parameters according to temperature.

~~In~~ A limitation of the previously mentioned studies ~~, the underlying idea is to first establish, when possible, a relationship between~~ linking rainfall extremes and ~~surface air temperature relying on data, and then to use temperature as a proxy to predict future rainfall extremes. Such reasoning relies on a strong assumption of sationarity in the physical processes generating rainfall, which may not be valid. This issue is not addressed in this work which focuses on exploring link between rainfall variability and extremes with temperature relying on current data. In general, this study also fits in this overall context by suggesting a different approach than that suggested by previously cited authors, with the aim of overcoming some of the previously reported limitations.~~

~~More precisely, a key observation is that there seems to be a strong scale dependence on the increase of rainfall extremes with temperature~~temperature is that only independent percentiles (or return periods) at a few independent observation scales are studied, without addressing the potential effects of the temperature on the rainfall process itself, i.e. the ~~increase seems stronger, and stronger than expected from CC relation only, for short durations (typically sub-hourly). A limitation of these studies is that only a few percentiles or a few return periods are studied, and not the whole~~ variability across scales ~~of rainfall fields~~is not investigated. In this paper, we suggest to ~~address the same issues as previously mentioned authors and to not focus on a few single observation scales independently as usually done, but to investigate how rainfall extremes and more generally~~ investigate more generally how rainfall variability across scales ~~, change~~ changes with temperature. This will enable to get more robust results in the sense that they are valid across a given range of scales. Indeed, rainfall is known to exhibit ~~scale invariant~~ scale-invariant features (see Lovejoy and Schertzer (1995) for an early review or Schertzer and Tchiguirinskaia (2020) for a more recent one), and relying on these features enables to suggest an innovative approach to explore the link

Table 1. Summary information for the various measurement campaigns during which the data used in this paper were collected.

Campaign name	Start date	End date	Number of days
ENPC Campus 1	08/01/2018	22/07/2020	927
ENPC Campus 2	14/10/2021	25/05/2025	1320
SIRTA	16/11/2016	19/09/2017	308
Pays d'Othes	11/12/2020	24/07/2023	956

between rainfall variability ~~, including extremes,~~ and temperature. More precisely, this paper ~~relies on~~ uses the framework of Universal Multifractals (UM). It is a physically based, mathematically robust framework which has been designed to analyze and simulate geophysical fields exhibiting extreme variability across a wide range of space-time scales such as wind or rainfall (see Schertzer and Tchiguirinskaia (2020) for a review). Such framework also enables to address the topic of rainfall extremes since the latter can be derived from underlying multifractal features.

The paper is structured as follows. In section 2, the data from three high resolution measurement campaigns over France is presented as well as the selection process of studied samples at large and event scales. Then the methodology, is presented with a recap of basic and needed multifractal properties, and a focus on the notion of maximum observable singularity. Finally, results at both large and event scales are discussed in section 4.

2 Data

2.1 Three measurement campaigns

Data collected during three measurement campaigns with devices operated as part of the Hydrology Meteorology and Complexity laboratory TARANIS observatory (exTreme and multi-scAle RAiNdrop parIS observatory) of the Fresnel Platform of École nationale des ponts et chaussées (https://hmco.enpc.fr/Page/Fresnel-Platform/en) are used. Summary information for each measurement campaign can be found in Tab. 1, and locations in Fig. 1.

The first campaign, called ENPC-Campus, takes place on the roof of the Carnot building on the campus of ENPC. In this paper, we use the rainfall data (only the rain rate in mm.h^{-1}) measured with the help of a Parsivel^2 disdrometer manufactured by OTT, and temperature obtained with the help of a sensor by Campbell Scientific. Both devices provide data with 30 s time steps. The corresponding data base, references presenting the devices, description of the campaign, as well as complete samples of data can be found in Gires et al. (2018). The rainfall and temperature time series used in this paper for the second part of ENPC-Campus campaign are displayed in Fig. 2 as an illustration of the studied data in this paper.

From November 2016 to September 2017 the instruments were moved to SIRTA (Site Instrumenté de Recherche par Télédétection Atmosphérique) on the Ecole Polytechnique campus for a joint intensive measurement campaign over the Ile-de-France

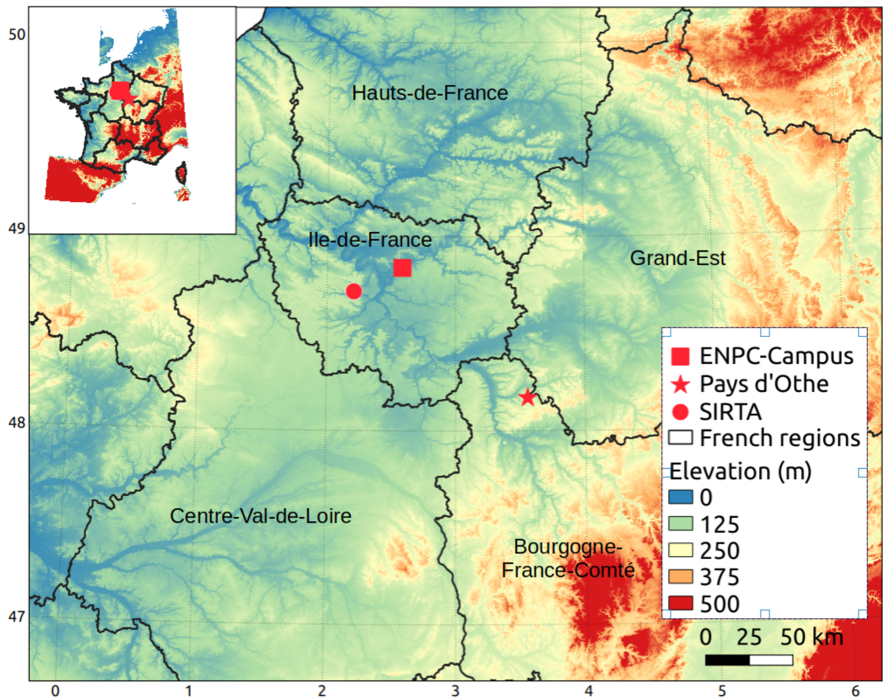

Figure 1. Location of the three measurement campaigns used in this paper. Coordinates system is ~~RGF93 Lambert 93~~ WGS84 (EPSG:~~2154~~4326)

region, where Paris is located. The site is about 38 km away from ENPC campus towards south west of Paris. This campaign is denoted SIRTA in this paper.

The last measurement campaign used in this paper took place at a wind farm operated by Boralex and located at Pays d'Othe (name of the campaign), approximately 120 km south east of Paris in a slightly ~~sloping~~ rolling area. As for the other campaigns, a Parsivel^2 disdrometer with 30 s time steps provided rainfall data. Temperature data ~~was~~ were collected with the help of a mini meteorological station manufactured by Thies Clima and operated with a sampling rate of 1 Hz. Temperature data was upscaled to 30 s time steps to match the resolution of the rainfall data. The devices were installed on a meteorological mast at a height of 45 m. Complete description of the campaign and samples of data can be found in Gires et al. (2022).

The whole rainfall and temperature time series used in this paper, from each measurement campaign, can be accessed in Gires (2025).

Measurement of rainfall with the help of optical disdrometers are subject to instrumental limitations, notably calibration issues and influence of wind (see Lanza et al. (2021) for a review). Observed deviations can go up to roughly 10 % (Capozzi et al., 2021), and some correction scheme (when wind data is available) have recently been suggested (Chinchella et al., 2024). Addressing these issues and the influence of the associated uncertainty on the multifractal analysis carried out would be an interesting topic, but it remains outside the scope of this paper.

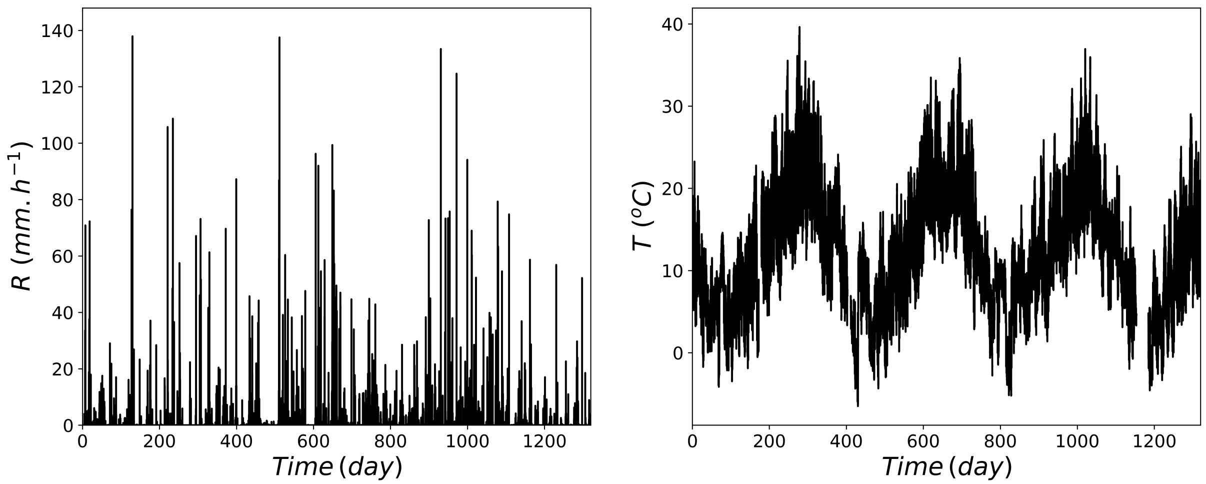

Figure 2. (Left) Time series of the rain rate during campaign "ENPC Campus 2". (Right) Time series of the temperature during campaign "ENPC Campus 2". 30 s time steps are used in both cases.

2.2 Sample selection at large scales

In a first step, ~~analysis~~ analyses are carried out up to synoptic scale, which corresponds to the typical duration of a large scale meteorological situation with typical temporal extent of up to 10 days and spatial extent of up to 1000 km. This scaling regime is called "large scales" in the rest of the paper.

More precisely, for each measurement campaign, the whole time series of rain ~~rates~~ rate and temperature are split into successive samples of 2^{15} time steps, which corresponds to roughly 11.4 days. The process is initiated at the beginning of the available data without accounting for potential ~~effect~~ effects of diurnal variations. The paper focuses on rainfall, so potential snowfall should be removed in order to avoid introducing potential biases. In order to achieve this, all samples for which some "rainfall" was recorded while the temperature for the same time steps was below 2 ^oC were simply removed from the studied set of samples. A more conservative threshold of 4 ^oC was not used to avoid discarding too much data that would correspond to rain. Hail is very rare in these locations, and filters for potential hail were not implemented. The total number of samples per measurement campaign can be found in ~~Appendix (Tab. ??)~~Tab. 1 of supplementary material. The total length of the studied samples corresponds to roughly 5.4, 0.7 and 2.0 years for the ENPC campus, SIRTA and Pays d'Othe measurement campaign respectively.

2.3 Sample selection at event scale

Analyses were also implemented at event scale. To achieve this, rainfall events were selected by considering that a rainfall event is a rainy period of time during which more than 1 mm is collected and that is separated by more than 15 min of dry time steps before and after. More precisely, in order to identify them, a rainy time step found after a dry period of at least

15 min is considered as start of a potential event. The end of the latter is the beginning of the next 15 min dry period. If the collected amount of rainfall is greater than 1 mm in between, then it is considered as a rainfall event. The number of events per measurement campaign can be found in ~~appendix (Tab. ??)~~Tab. 2 of supplementary material. As for the large ~~scale~~ scales analysis, events for which the average temperature was lower than 2 ^oC were discarded (see ~~appendix~~ supplementary material for numbers of events kept in analysis), in order to avoid potential biases associated with snowfall.

The selected rainfall events do not all have the same duration. Hence, a sample length is set for further joint analysis of the events. For technical reasons (see next section), it must correspond to a power of 2 of ~~the~~ number of time steps. Longer sample lengths enable to study rainfall across a wider range of scales, getting more robust results; but they impose to discard shorter events. Shorter sample lengths enable to keep a maximum of rainfall events; but limit the robustness of the results, being obtained across a more limited range of scales. As a trade-off, a sample length of 128 time steps corresponding to 64 min ($\sim$ 1h) was used. Then, in order to study the maximum possible data, the process illustrated in Fig. 3 was implemented for each event: (i) the maximum number of sub-events, i.e. non overlapping samples of size 128, was computed. It is equal to the integer part of the number of time steps of the event divided by 128 (ii) In order to study as much rainfall as possible, the portion of length equal to the product of number of samples ~~time~~ times 128 with highest cumulative depth was found within the time series of the event. Given that disdrometer measurements were given at drop scale, there is a unique maximum. (iii) This selected portion was finally split into sample(s).

3 Methodology

3.1 Universal Multifractal framework

In this paper, variability and ultimately extremes of the rainfall ~~fields~~ times series across various ranges of scales, were quantified in the framework of Universal Multifractals (UM). Here, only the key elements are reminded and interested readers are referred to a recent review by Schertzer and Tchiguirinskaia (2020) and references therein for more details.

To introduce the framework, let us consider a conservative (i.e. its average does not change with scales) ~~field~~ 1D time series ϵ_λ at a resolution λ. It is defined as the ratio between the outer scale (~~T~~T_{out}) and observation scale (~~t~~T_{obs}), i.e. ~~$\lambda = T/t$. The word "field" can refer in general to processes in 1D, 2D or more; yet in this work, only~~ $\lambda = T_{out}/T_{obs}$. For multifractal 1D ~~processes corresponding to time serieswere analysed. For multifractal fields~~time series, the moment of order q of the ~~field~~ series exhibits a power law relation with regard to the resolution:

$$\langle \epsilon_\lambda^q \rangle \approx \lambda^{K(q)} \tag{1}$$

where $K(q)$ is the scaling moment function. The notation $\langle . \rangle$ denotes the average ~~of the field~~over the time series. It can be shown that, in an equivalent way, the probability of exceeding a scale dependent threshold (λ^γ) defined with the help a ~~scale invariant~~ scale-invariant singularity γ, also scales with the resolution as:

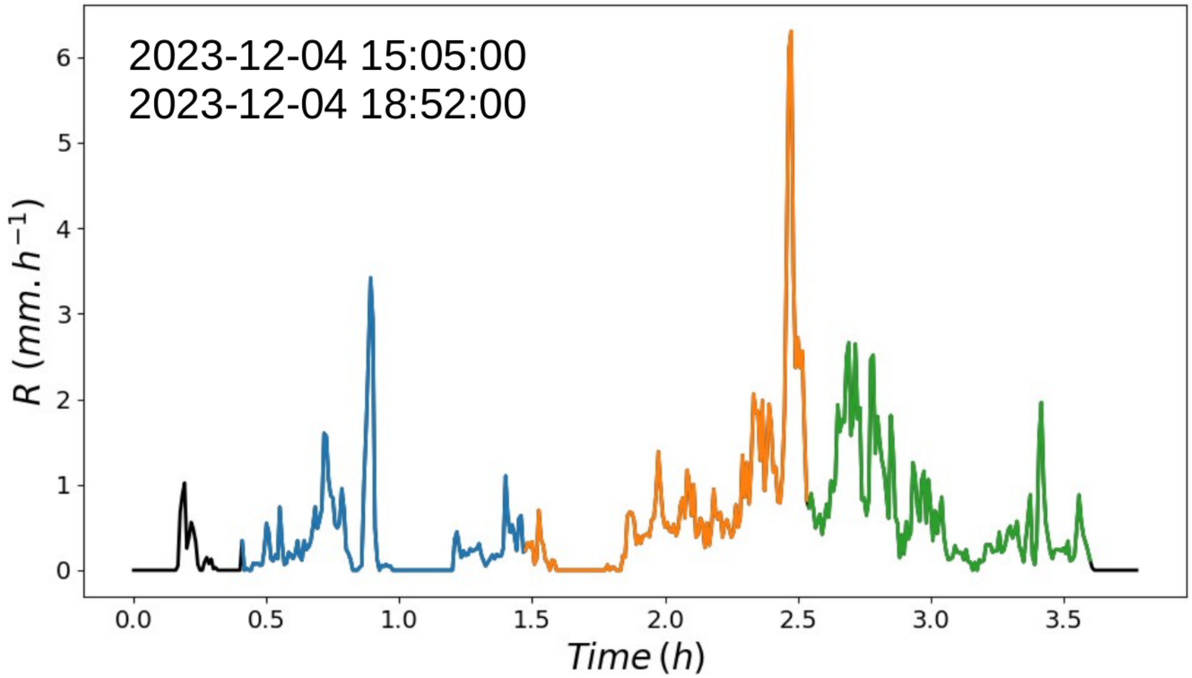

Figure 3. Illustration of how samples of 128 time steps (64 min) were extracted from a rainfall event that was collected during the ENPC-Campus campaign. In that case, three samples were extracted.

$$Pr(\epsilon_\lambda \geq \lambda^\gamma) \approx \lambda^{-c(\gamma)} \tag{2}$$

where $c(\gamma)$ is the codimension function (Schertzer and Lovejoy, 1987). ~~A multifractal field behaves~~ The values of multifractal 1D time series behave as λ^γ. The singularity (γ) remains the same across scales while the value of the ~~field~~ time series (λ^γ) changes with scales. The functions $K(q)$ and $c(\gamma)$ fully characterize the variability across scales of the ~~field~~ time series ϵ_λ and are linked ~~by~~ through a Legendre transform (Parisi and Frisch, 1985). This notably means that a singularity can be associated uniquely to each moment and vice-versa. Eqs. 1 and 2 also mean that multifractal properties are statistical properties which are valid on average over numerous samples.

In the specific framework of UM (Schertzer and Lovejoy, 1987), which are a limit behaviour of all multiplicative cascades processes (see discussion in Schertzer and Lovejoy (1997) for more details on this debates), $K(q)$ and $c(\gamma)$ are characterized with the help of only two parameters with physical interpretation:

- C_1, the mean intermittency co-dimension, which measures the clustering of the (average) intensity at smaller and smaller scales. $C_1 = 0$ for ~~an~~ a homogeneous field;

- α, the multifractality index ($0 \leq \alpha \leq 2$), which measures the clustering variability with regard to the intensity level.

Greater values of α and C_1 correspond to stronger extremes. For UM, we have:

$$K(q) = \frac{C_1}{\alpha - 1}\left(q^{\alpha} - q\right). \tag{3}$$

A Trace Moment (TM) analysis basically consists in checking the scaling behaviour of the ~~field~~ time series and estimating $K(q)$ by plotting Eq. 1 in log-log. To achieve this, the ~~field~~ time series is upscaled from its maximum resolution Λ by averaging over adjacent time steps, then raised to various powers q, and finally the ensemble average (over various samples independently upscaled) is performed to obtain an estimate of the empirical moments and their scaling behaviour. UM parameters are estimated with the help of the Double Trace Moment ~~techniques~~ technique which is an extension of TM tailored for UM (Lavallée et al., 1993).

Let us now consider a non-conservative ~~field~~1D time series, denoted ϕ_λ, whose average changes with scales, i.e. we have $\langle \phi_\lambda \rangle \neq 1$. In that case, it is usually assumed that it can be written as (with an equality in probability distribution):

$$\phi_\lambda \overset{d}{=} \epsilon_\lambda \lambda^{-H} \tag{4}$$

where ϵ_λ is a conservative ~~field~~ time series ($\langle \epsilon_\lambda \rangle = 1$) of moment scaling function $K_c(q)$ (the sub-index “c” refers to the conservativity of ϵ_λ), and H the non-conservation parameter. $K_c(q)$ only depends on UM parameters C_1 and α. H characterizes the scale dependence of the average ~~field~~behaviour, and is equal to zero for a conservative ~~field~~time series. H should not be confused with the Hurst exponent: although both quantify long-range correlations for values greater than zero, the latter lacks a simple general expression for multifractal processes (more details can be found in appendix A of Jose et al. (2024a)).

H ~~can easily be~~ is related to spectral analysis. Indeed, for scaling ~~fields~~time series, the power spectrum follows a power law with regard to wave number:

$$E(k) \approx k^{-\beta} \tag{5}$$

and the spectral slope β is related to H with the help of the following formula (Tessier et al., 1993):

$$\beta = 1 + 2H - K_c(2) \tag{6}$$

TM and DTM ~~technique~~ techniques should theoretically be implemented on a conservative ~~field~~ time series ϵ_λ. However if H is roughly smaller than 0.3-0.4, it can be implemented directly on ϕ_λ, without substantially biasing the estimates of α and C_1. In case of greater H, ϵ_λ should be used in the TM and DTM technique. Retrieving ϵ_λ from ϕ_λ theoretically requires a fractional integration of order H (equivalent to a multiplication by kH in the Fourier space). A common approximation, which provides reliable results, consists in taking ϵ_Λ as the absolute value of the fluctuations of ϕ_Λ at the maximum resolution and renormalizing it (Lavallée et al., 1993).

3.2 Maximum observable singularity

The insight one can get of a statistical process is limited by the size of the studied sample. For multifractal processes, this will result in a maximum singularity γ_s and corresponding moment order q_s beyond which the values of the statistical estimates of respectively the codimension and scaling moment functions are not considered as reliable (e.g., Lovejoy and Schertzer, 1989, 2007).

More precisely, let's consider N_s independent samples with a resolution λ. In a d-dimensional space, there are λ^d values per sample ($d = 1$ for the time series studied in this paper). The maximum singularity (γ_s) that one can expect to observe in the available samples is defined by:

$$N_s \lambda^d Pr(\epsilon_\lambda \geq \lambda^{\gamma_s}) \approx 1 \tag{7}$$

Introducing the notion of sampling dimension d_s: $N_s = \lambda^{d_s}$ ($d_S = 0$ for a single sample as it will be the case here), it yields:

$$c(\gamma_s) = d + d_s \tag{8}$$

which enables to estimate γ_s. For $\gamma > \gamma_s$ one expects that $c(\gamma) = +\infty$, which means that the estimates of $c(\gamma)$ will not be reliable. As a consequence of the Legendre transform, the empirical estimates of $K(q)$ ~~becomes~~ become linear for $q > q_s = c'(\gamma_s)$: $K(q) = \gamma_S(q - q_s) + K(q_s)$. γ_s quantifies in a scale-invariant way the extremes that can be expected within a time series. The corresponding physical quantity at a given resolution λ is expressed as λ^{γ_s}. It is especially useful to quantify how extremes evolve when α and C_1 exhibit different trends. Indeed, γ_s combines the influence of both UM parameters into a single one. For example, Royer et al. (2008) ~~analysed~~ analyzed rainfall output of climate models over France and found decreasing trend for α and increasing one for C_1. Relying on the notion of maximum observable ~~, They showed that , as a combined effect,~~ which combines the effects of both parameters, they showed that rainfall extremes are expected to increase over France in the context of climate change. Douglas and Barros (2003) used it to discuss the concept of maximum probable rainfall. Qiu et al. (2024) relied on this tool to quantify the impact of rainfall space-time variability on the usefulness of nature-based solutions in urban environment.

4 Results

4.1 Large ~~scale~~scales

In this subsection, we implemented multifractal ~~analysis~~ analyses on large scales, i.e. up to synoptic scale (see section 2.2). In a first step, an ensemble analysis was carried out, that is to say all samples were upscaled independently and used to compute average statistical moments in Eq. 1 or spectra in Eq. 5. Such analysis is used to study general features of scaling.

Let us illustrate the results with the ENPC-Campus campaign. ~~Outcome~~ The outcome of spectral analysis, i.e. Eq. 5 in log-log, is displayed in Fig. 4.a. An excellent scaling behaviour on scales ranging from roughly 30 min to 11 days is found,

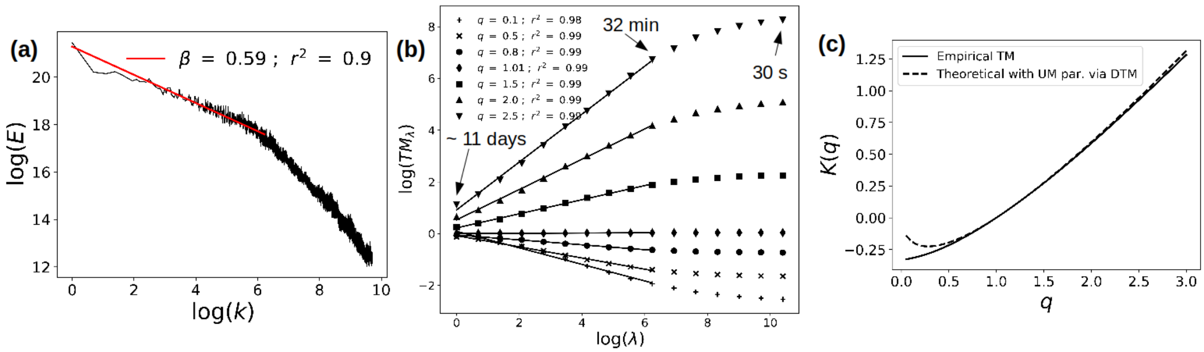

Figure 4. For the campaign "ENPC campus" with ensemble analysis for large scales. (a) Spectral analysis, i.e. Eq. 5 in log-log. (b) TM analysis, i.e. Eq. 1 in log-log. (c) Scaling moment function $K(q)$: empirical estimate and theoretically fitted shape using UM parameters from DTM analysis.

and smaller scales are investigated in next subsection. The spectral slope β is smaller than 1, meaning that across this range of scales the studied ~~field~~ time series is conservative and multifractal analysis can be implemented directly on the ~~field~~time series. Trace Moment analysis (i.e. Eq. 1 in log-log) outcome is displayed in 4.b. The coefficients of determination of the linear regressions are all greater than 0.99 for $q > 0.5$ and we ~~used~~ use the one for $q = 1.5$ as a metric. Results confirm the excellent scaling behaviour across this range of scales.

UM parameters estimated with the help of DTM technique are reported in Tab. 2. In the DTM technique, moments ranging from 1.1 to 1.5 are tested enabling to provide an uncertainty range on the estimates of UM parameters. The latter is very small compared to the differences between sites (and samples in upcoming analysis), so it will not be discussed further. UM parameters values are typical for this range of scales (e.g., Ladoy et al., 1993; de Lima and Grasman, 1999). ~~An excellent agreement is retrieved when comparing the~~ The empirical scaling moment function $K(q)$ derived from TM analysis and the theoretical one plotted using Eq. 3 and DTM estimates of UM parameters ~~(~~are is excellent agreement as it can be seen visually in Fig. 4.c~~)~~. The discrepancies ~~that can be noticed~~ noticeable for $q < 0.5$ are explained by a multifractal phase transition associated with the numerous zeros which are in the time series (see Gires et al. (2012) for more details on this phenomenon). Very small values of H (last column of Tab. 2), i.e. smaller than 0.1, corresponding to almost conservative ~~field~~time series, are retrieved for this range of scales.

Same excellent scaling behaviour was observed for this range of scales for the two other measurement campaigns. Similar UM parameters were retrieved with only limited variations of α and C_1 (see Tab. 2) according to the campaign.

In a second step, in order to investigate how UM features are changing with temperature, the average temperature $< T >$ for each sample was computed from the available data~~, and~~. Even if the temperature also exhibits some variability, only the average temperature was considered. Joint multifractal analyses could be envisaged in future studies (e.g. Jose et al., 2024b). Then, two types of ~~analysis~~ analyses were carried out:

– Individual sample analysis.

Table 2. Summary of UM parameters assessed across large scales (32 min - 11 days) using ensemble analysis for each measurement campaign

Campaign name	r^2	α	C_1	β	H	γ_s
ENPC Campus	0.997	~~0.611~~ 0.61 ± 0.0022	~~0.490~~ 0.49 ± 0.0022	~~0.594~~ 0.59	0.094	3.21
SIRTA	0.996	~~0.623~~ 0.62 ± ~~0.0136~~ 0.013	~~0.495~~ 0.49 ± 0.0047	~~0.530~~ 0.53	0.067	3.09
Pays d'Othe	0.997	~~0.669~~ 0.67 ± 0.0068	~~0.484~~ 0.48 ± 0.0040	~~0.547~~ 0.55	0.073	2.96

– Ensemble analysis of samples within a given range of temperature.

In the first type of analysis, a UM analysis was implemented on each sample individually using the same range of scales that was identified in the ensemble analysis. Individual samples with bad scaling, i.e. with $r^2 < 0.9$ for $q = 1.5$ were discarded (see ~~appendix~~ supplementary material for numbers of samples kept in the analysis) from this analysis. Scaling being an average behaviour, it is expected that some samples do not exhibit a good scaling behaviour. And they were incorporated in the ensemble analysis before and the binned one after. Yet, adding their assessed parameters in the individual analysis would not be relevant because they are not reliable so they could bias results. Scatter plots of retrieved UM parameters vs. $< T >$ are displayed in Fig. 5 for ENPC-Campus campaign. Significant scattering is observed for all parameters. Potential overall trends were identified with the help of a simple linear regression. It is displayed through the red line on the plots. The quality of the linear regression was quantified with the help of the Pearson coefficient of correlation, denoted r. It ranges from -1 (exact linear relationship with negative slope) to 1 (exact linear relationship with positive slope). Values close to 0 correspond to lower level of correlation. As a complement, Pearson p-value was computed in order to test the null hypothesis that the distribution of the underlying samples are uncorrelated. A threshold of 0.05 was used to reject the null hypothesis. Assessed slopes and Pearson coefficients of correlation r along with associated level of confidence are displayed in Tab. 3.

The $|r|$ coefficients are low, which is expected given the observed scattering. It means that the retrieved trends are only valid on average over numerous events, and they are not all statistically significant. For example, for H none of the observed trends for individual campaign pass the statistical test of significance. Also, in the case of the SIRTA campaign, there are not enough samples to get statistically reliable trends. We observed a decreasing trend for α and an increasing trend for C_1. Hence the consequences on extremes were not obvious and γ_s was needed to combine the effects of both. It appears that γ_s exhibits an increasing trend with $< T >$. It means that stronger variability and extremes are retrieved on studied samples with increasing temperature. A slightly decreasing trend is found for β and very slightly decreasing one for H.

In the second type of analysis, the temperature range from 2 to 24 ^oC was split into bins of 2 ^oC width. Then, an ensemble analysis of all the samples whose average temperature is ~~withing~~ within a given bin was performed. Some precision is lost with regard to temperature, but it enables to get more robust scaling, which is an average feature valid on numerous samples. Given that UM features from the various campaign were very similar and in order to increase the number of samples to obtain more reliable results, all the available samples from all the campaigns were used. Results are displayed in Fig. ~~??~~ ?? in red for the

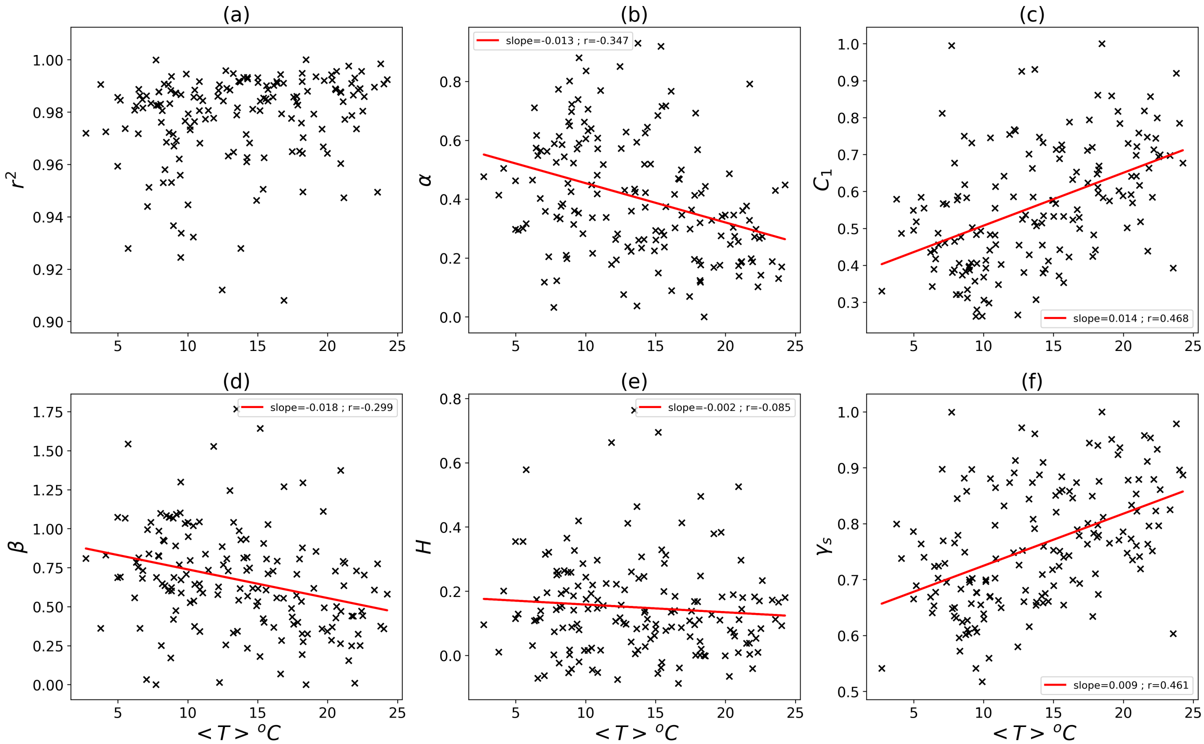

Figure 5. For the campaign "ENPC campus" with individual sample analysis for large scales: r^2 for $q = 1.5$ in TM analysis (a), α (b), C_1 (c), β (d), H (e) and γ_s (f) vs. $<T>$

Table 3. Slope ($\times 10^{-2} {}^\circ C^{-1}$) (corresponding Pearson coefficient of correlation r, in bold if the null hypothesis of no trend was rejected) of the linear regression of the value of the studied parameter vs. $<T>$ (individual sample analysis) at large scales. Illustration in Fig. 5 for "ENPC" Campus campaign.

Campaign name	α	C_1	β	H	γ_s
ENPC Campus	-1.34 (~~**-0.348**~~**-0.35**)	1.43 (~~**0.469**~~**0.47**)	-1.83 (~~**-0.299**~~**-0.30**)	-0.24 (~~-0.0857~~-0.086)	~~0.931 (~~0.93 (~~**0.461**~~**0.46**)
SIRTA	~~0.592 (0.174~~0.59 (0.17)	0.090 (0.0034)	-2.27 (~~-0.343~~-0.34)	-1.09 (~~-0.366~~-0.37)	~~0.246 (0.141~~0.24 (0.14)
Pays d'Othe	~~-0.968 (-0.234~~-0.97 (-0.23)	1.21 (~~**0.350**~~**0.35**)	-2.31 (~~**-0.336**~~**-0.34**)	~~-0.568 (-0.185~~-0.57 (-0.18)	~~0.884 (~~0.88 (~~**0.375**~~**0.37**)
All	-1.05 (~~**-0.272**~~**-0.27**)	1.23 (~~0.394~~0.39)	-2.02 (~~**-0.316**~~**-0.31**)	~~-0.414 (~~-0.41 (~~**-0.143**~~**-0.14**)	~~0.854 (~~0.85 (~~**0.409**~~**0.41**)

large ~~scale~~ scales studied in this subsection. First of all, the scaling (r^2) is very good for all temperature bins. First and second bins were not accounted for in the linear regression because of too low number of samples (1 and 4 respectively compared to more than 14 for all the others; see Tab. ~~?? in appendix~~3 in supplementary material) with regard to the other bins. A larger data

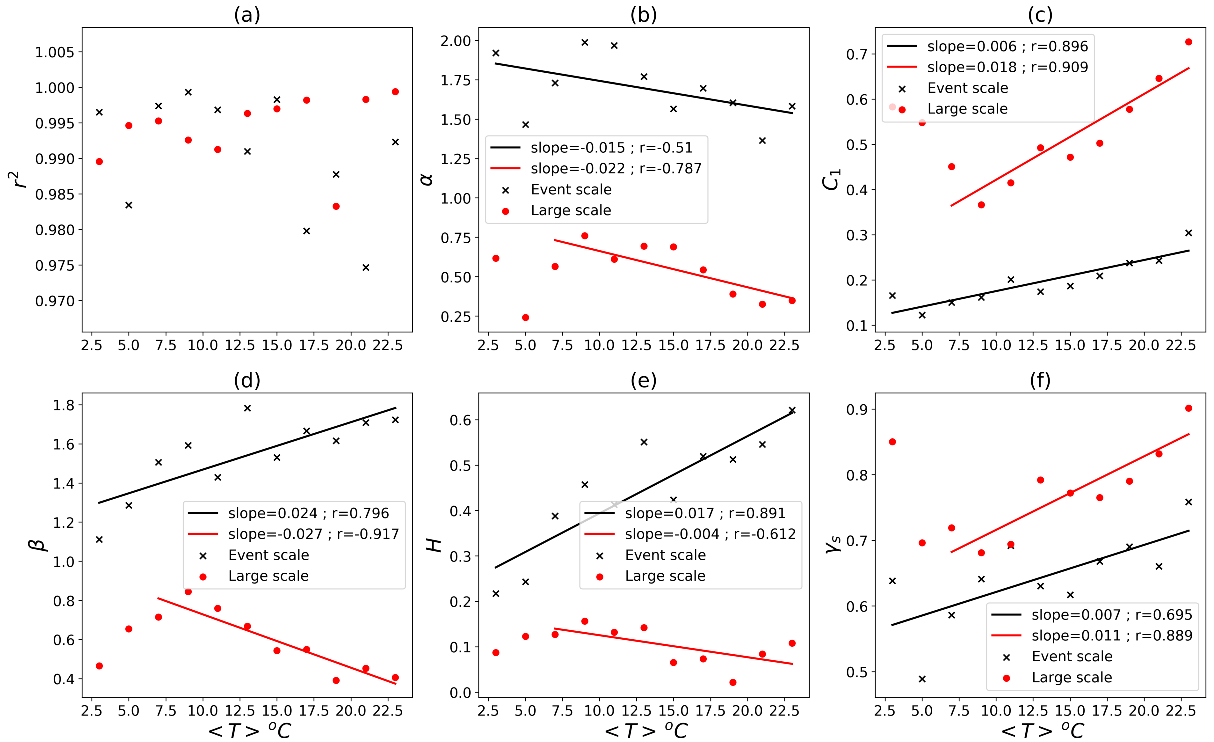

Figure 6. For all the ~~campaigned~~ campaign merged together and samples binned within classes of temperature of 2^oC width: $r2$ for $q = 1.5$ in TM analysis (a), α (b), C_1 (c), β (d), H (e) and γ_s (f) vs. $< T >$

set would enable to explore wether this trend is real and associated with changes of precipitation type with temperature. The linear trends computed do not account for the unequal number of samples per bin. The same trends that were obtained with the previous analysis are retrieved, i.e. α, β and H decrease with $< T >$, while C_1 and γ_s ~~increases~~increase. The obtained trends are more robust than in the previous analysis as confirmed by the much higher coefficients of correlation.

4.2 Event scale

In this subsection, analysis were carried out at event scale (see section 2.3). The same analysis as for longer samples across large scales were carried out, with ensemble analysis first, to identify scaling behaviour, and then individual sample analysis in two formats.

Results are illustrated with the data from ENPC-Campus campaign. Spectral analysis (Fig. 7.a) shows that data exhibits a very good scaling behaviour on the whole range of scales from 30 s to 1 h. The spectral slope β is of 1.73 meaning that on this range of scales, the studied ~~field~~ time series is not conservative, i.e. there are some strong long range correlations. Hence the analysis is done on the conservative part (see section 3.1). Fig. 7.b shows TM analysis. The excellent scaling behaviour on the whole range of studied scales (30 s - 64 min) is confirmed, with coefficients of determination all greater than 0.99 for $q > 0.5$.

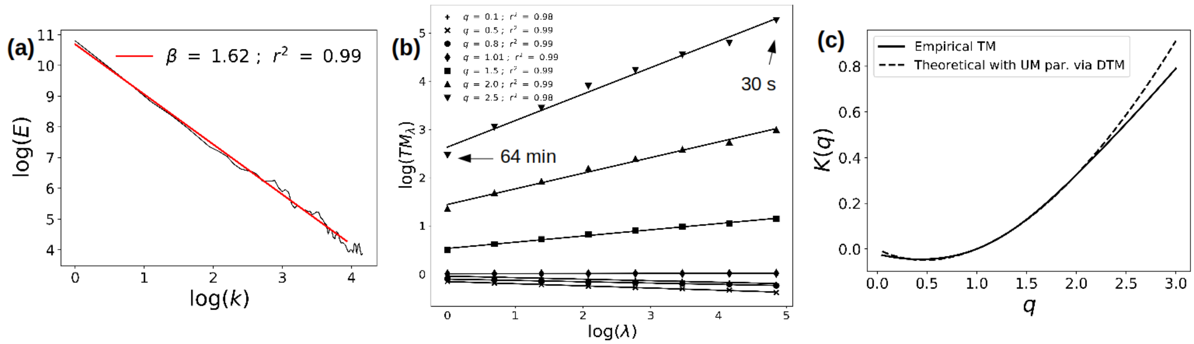

Figure 7. For the campaign "ENPC campus" with ensemble analysis at event scale. (a) Spectral analysis, i.e. Eq. 5 in log-log. (b) TM analysis, i.e. Eq. 1 in log-log. (c) Scaling moment function $K(q)$: empirical estimate and theoretically fitted shape using UM parameters from DTM analysis.

Table 4. Summary of UM parameters assessed at event scale (30 s - 64 min) using ensemble analysis

Campaign name	r^2	α	C_1	β	H	γ_s
ENPC Campus	0.994	1.74 ± 0.0082	~~0.180~~ 0.18 $\pm$ 0.0023	1.63	~~0.478~~ 0.48	2.69
SIRTA	0.988	1.76 ± 0.011	~~0.189~~ 0.19 $\pm$ 0.0026	1.50	~~0.421~~ 0.42	2.58
Pays d'Othe	0.995	1.88 ± 0.012	0.206 ± 0.0031	1.52	~~0.459~~ 0.46	2.32

UM parameters obtained via DTM analysis are in Tab. 4. These values, around 1.7-1.8 for α and 0.2 for C_1, are consistent with those commonly reported in the literature for this range of scales (e.g., Gires et al., 2016; de Montera et al., 2009; Mandapaka et al., 2009; Verrier et al., 2010; Jose et al., 2024b). Similarly to the large scale analysis of previous section, the uncertainty on UM parameters estimates is very small compared to the differences observed between measurement campaigns and in between samples as we will see. Hence this will not be further accounted for. As for the results across large scales, there is a very good agreement between the empirical scaling moment function $K(q)$ and the theoretical one. Some differences become visible for $\cancel{q \approx 2.3 - 2.5}$ q greater than $\approx 2.3 - 2.5$ which is slightly smaller than the expected value of q_s equal to 2.7 in this case.

Very similar qualitative and quantitative (see Tab. 4) were retrieved on this range of scales for the two other measurement campaigns.

As for the large scales in the previous section, the average temperature $< T >$ over the whole event was assessed for each event, and the same two types of UM ~~analysis~~ analyses on individual events (the sample(s) of a same event are analyzed together) and ensemble of events binned by temperature intervals were carried out.

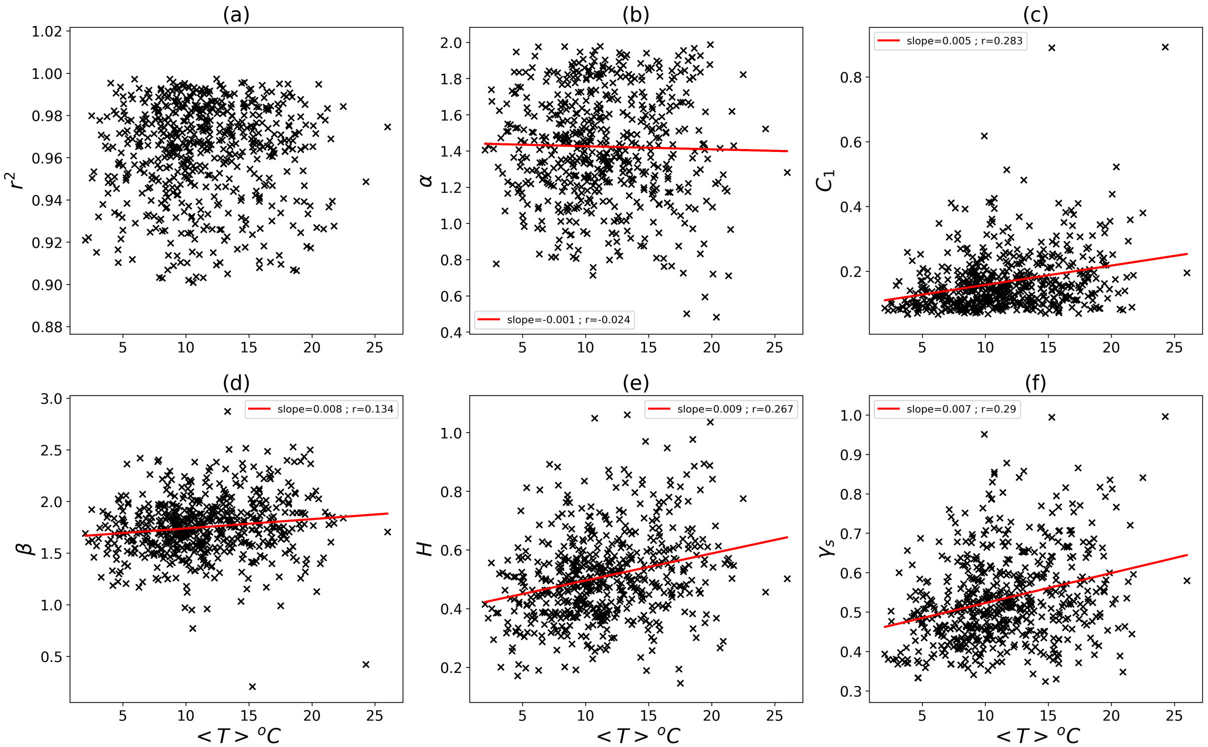

Figure 8. For the campaign "ENPC campus" with individual sample analysis at event scale: r^2 for $q = 1.5$ in TM analysis (a), α (b), C_1 (c), β (d), H (e) and γ_s (f) vs. $< T >$

As before and for the same reasons, ~~in~~ the individual events with bad scaling, i.e. with $r^2 < 0.9$ for $q = 1.5$, were discarded (see ~~appendix~~ supplementary material for numbers of samples kept in analysis). Scatter plots of retrieved UM parameters vs. $< T >$ are displayed in Fig. 8 for ENPC-Campus campaign. Stronger scattering than for the large scales is retrieved. Similarly potential overall trends were computed with the help of linear regressions. Slopes and r and p-value are reported in Tab. 5 for all measurement campaigns.

In general similar results but with less pronounced trends (smaller $|r|$) are retrieved for UM parameters with a slightly decreasing α, an increasing C_1 and an increasing γ_s. It means that ~~extremes and variability~~ variability and extremes also tend to increase with temperature over this range of scales. Contrarily to what is observed at large scales, β and H are increasing with temperature, corresponding to a greater non conservativeness of the ~~field~~time series.

Results for the binned analysis are displayed in Fig. 6 in black. As in the case of the large ~~scale~~scales, they basically confirm the results discussed in the previous paragraph in a more robust way.

Table 5. Slope ($\times 10^{-2} {}^{\circ}C^{-1}$) (corresponding Pearson coefficient of correlation r, in bold if the null hypothesis of no trend was rejected) of the linear regression of the value of the studied parameter vs. $< T >$ (individual event analysis) at event scale. Illustration in Fig. 5 for "ENPC" Campus campaign.

Campaign name	α	C_1	β	H	γ_s
ENPC Campus	~~-0.170 (-0.0243~~-0.17 (-0.024)	~~0.597 (~~0.60 (**~~0.283~~0.28**)	~~0.897 (~~0.90 (**~~0.134~~0.13**)	~~0.922 (~~0.92 (**~~0.267~~0.27**)	~~0.761 (~~0.76 (**~~0.29~~**
SIRTA	-1.39 (~~-0.203~~-0.20)	~~0.587 (~~0.59 (**~~0.402~~0.40**)	1.60 (**~~0.307~~0.31**)	1.20 (**~~0.463~~0.46**)	~~0.664 (~~0.66 (**~~0.31~~**
Pays d'Othe	-1.15 (**~~-0.167~~-0.17**)	~~0.346 (~~0.35 (**~~0.171~~0.17**)	1.82 (**~~0.251~~0.25**)	1.11 (**~~0.301~~0.30**)	~~0.285 (0.107~~0.29
All	~~-0.592 (~~-0.59 (**~~-0.0854~~-0.085**)	~~0.508 (~~0.51 (**~~0.250~~0.25**)	1.31 (**~~0.193~~0.19**)	1.03 (**~~0.298~~0.30**)	~~0.589 (~~0.59 (**~~0.22~~**

4.3 Seasonal and rainfall intensity sensitivity

Until now, all the analysis carried out account for events all around the year. In order to explore potential seasonal sensitivity, the same analysis was implemented considering the events for each season separately. The events / samples for which start month are December, January and February were labeled as winter. ~~In a similar~~ Similarly, the others were classified in spring (March, April, May), summer (June, July, August) and autumn (September, October, November). Slopes, as well as indicators of the quality of the linear regression of the value of the studied parameters vs. $< T >$ at both large and event ~~scale~~ scales for all measurement campaigns are displayed in Fig. 9. During winter, for large scales, $< T >$ for all samples ranged from 2.7 to 11 ^{o}C with a average values of 7.3 ^{o}C. Those numbers are equal to 7.3, 20 and 13 for spring, 15, 20 and 24 for summer and 2.8, 13 and 22 for autumn.

The "All" column corresponds to the results on average considering all the events of year, which were discussed in the previous two sections. With regard to results according to seasons, it should first be mentioned that they are less statistically reliable, and this is notably due to the fact that the number of samples / events was lower (roughly divided by 4) than when all events were considered at once. Yet, it seems that some trends are visible. For example for γ_s at large scales, it appears that there is a slight decrease of it with increasing temperature, while the trend discussed in previous subsection is valid for the other seasons. This effect is less pronounced at event scale. β also seems to behave differently in winter for large scales (except for the SIRTA campaign for which there is a limited number of samples available). Longer time series would be needed to further confirm these preliminary observations.

In addition to these ~~analysis~~analyses, sensitivity to rainfall intensity and temperature were tested. More precisely, same analysis considering only the events or samples with average rain rate belonging ~~in~~ to the 10 % upper percentile was carried out. Using the available data, no significant differences were found. An analysis splitting the events between those with average temperature below and above 12 ^{o}C also did not yield any significant differences. Studies on more events and other geographical areas would be needed to further investigate this, because other work found a dependency of the increase rate

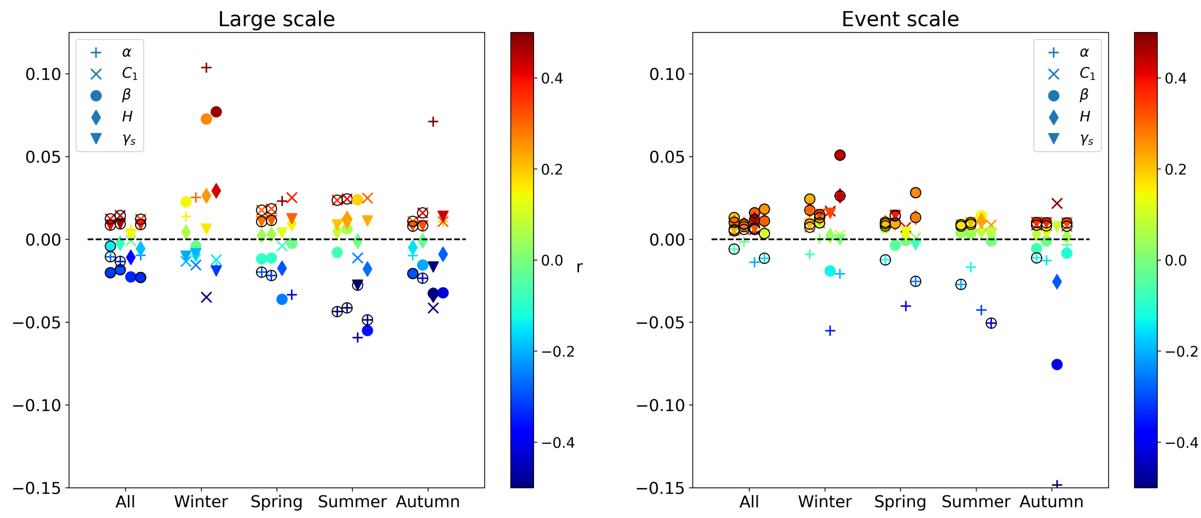

Figure 9. Slope ($°C^{-1}$) of the linear regression of the value of the studied parameters vs. $< T >$ at both large and event ~~scale~~ scales for each measurement campaign for all events (left, it corresponds to values displayed in Tab. 3 and 5) as well as per season. For each season, the 4 "columns" correspond in that order to all campaigns together, ENPC Campus, SIRTA and Pays d'Othe. Symbols are colored according to Pearson coefficient of correlation. The ones circled correspond to cases for which the null hypothesis of no trend was rejected.

with temperature (e.g., Lenderink and van Meijgaard, 2008; Chagnaud et al., 2024) ~~As mentioned in the introduction~~ Indeed, some authors reported more pronounced trends when considering high or low temperature range or only the upper percentiles of rainfall extremes. Longer time series, enabling to study more samples / events would be needed to implement this methodology to check whether similar effects are also found ~~. Further analysis~~ in this scale-invariant framework. Further analyses with longer time series and ~~climates, enabling to test the sensitivity to rainfall type, as for example differences between stratiform and convective situations~~various climate types, would be interesting to ~~check~~ carry out, to check for example how the extremes behave depending on rainfall ~~type~~ types, i.e. stratiform vs. convective situations for example (e.g., O'Gorman, 2015).

4.4 Link with other studies

The ~~analysis~~ analyses carried out did not aim at determining whether a super-CC or sub-CC is observed, since ~~it focused on extreme variability~~ they focused on variability in general. Yet, given that rainfall extremes can be derived from some multifractal features, it is possible to relate the current results to previous findings available in the literature. More precisely, as discussed in the introduction, numerous studies have reported a scale dependence of the increase of rainfall extremes with temperature, i.e. that the increase is stronger in percentage for shorter durations (Fowler et al., 2021; Haerter et al., 2010; Lenderink and van Meijgaard, 2008; Lenderink et al., 2017; Panthou et al., 2014). Results presented here, provide a framework to interpret this.

In this study we find in general an increase of the scale invariant concept of maximum observable singularity γ_s of rainfall time series with temperature~~, as expected with CC relationship. The rainfall extreme~~. γ_s being related to the extreme rainfall (greater γ_s corresponds to stronger extremes), one can note that, at least for small scales, it is consistent with previous findings from the literature reporting an increase of rainfall extremes with temperature. It is even possible to go a step further and explore how this increase is expected to change with observation scale. Indeed, the greater rainfall rate (i.e. an indicator of extreme rainfall) that one can expect to observe in a sample at resolution λ behaves as λ^{γ_s}. We remind that λ is the resolution, i.e. the ratio between the outer scale and the observation scale, and that it increases with shorter duration. Hence, an increase of the scale invariant γ_s with temperature results in greater increase of extreme rainfall in percentage at higher ~~resolution~~resolutions, i.e. with shorter observation scales. Indeed, this percentage of increase $\%_{incr}$ can be written as:

$$\%_{incr} = 100 \times \left(\lambda^{\gamma_s(T_1)-\gamma_s(T_2)} - 1\right) \tag{9}$$

for a change from temperature T_1 to T_2. Hence the change with temperature in the scale invariant parameter γ_s provides a framework to explain changes in increase of rainfall extremes with temperature according to scale (mainly from ~~hourly to daily~~ daily to hourly) which were reported in previous studies. Indeed, with $\gamma_s(T_1) - \gamma_s(T_2)$ fixed in Eq. 9 (i.e. the increase of γ_s with temperature), when λ increases (i.e. shorter durations are considered), the percentage of increase of the expected rainfall extreme rises. Let us consider an illustration with a temperature shift of 2 ^{o}C for the large scales. It corresponds to a shift of γ_s equal to 0.0085×2 (Tab. 3). T_{out} here is 11 days as shown in the multifractal analysis. At daily scale T_{obs} is one day. This yields to $\lambda = 11/1$ which gives an increase of the maximum expected rainfall of roughly 4%. At hourly scale T_{obs} is one hour, leading to $\lambda = 11/(1/24)$ and an increase of roughly 10% on expected maximum rainfall. This shows that relying on a scale invariant framework enables to grasp an understanding valid across a given range of observation scales. This constitutes a novelty with regard to previous studies.

5 Conclusions

In this paper, we studied how rainfall extremes and more generally variability across scales changes with temperature. For this, we used data coming from three high resolution measurement campaigns that took place in France between 2018 and 2025; and we relied on the framework of Universal Multifractals. More precisely, we first confirmed scaling behaviour and then estimated UM parameters α, C_1, the corresponding maximum observable singularity γ_s, and H for each sample and studied their dependence to temperature.

It appeared that for scales ranging from 32 min up to the synoptic scale of roughly 11 days, an excellent scaling behaviour was retrieved and we observe a decrease of α with average temperature, an increase of C_1 which ~~yielded an~~ yields an overall increase of γ_s. There was a slight decrease of H. Similar trends but less pronounced were observed at event scale, i.e. for scales ranging from 30 s to roughly 1 h, for α, C_1 and γ_s. On the contrary, an increasing trend with average temperature was found for H.

This increase of γ_s with temperature confirms previous findings of expected increase of rainfall extremes with temperature. It confirms them in a scale invariant way and ~~enables~~ helps to explain the dependence of the rate of increase with observation scale that is reported in previous studies.

Consistent results were found here between event and large scales and over three measurement campaigns. It suggests that findings are robust. Yet, the three stations used are located in a small meteorological region at planetary scale. It would definitely be relevant to expand the analysis to much wider areas using data from various climates to expand our understanding ~~on~~ of the dependence of rainfall extremes with temperature. It would notably enable to explore temperature range greater than $23\ ^oC$ which is the maximum available with data set studied in this paper. Investigating the geographical dependence of the rate of change of UM parameters with temperature would notably be insightful and should be pursued in upcoming studies. It would also be very interesting to carry out similar analysis on the output of climate models, which are commonly used to investigate how rainfall extremes will change (e.g., Li et al., 2019; Dallan et al., 2024; Chagnaud et al., 2024). They notably enable gridded analysis to explore in details longer time series as well as spatial patterns on the retrieved results, and could also help in overcoming issues like potential changes in the circulation regime. A major advantage of using model outputs is also the possibility to explore spatial extremes, i.e. how these results remain valid for various spatial scales, which is an important issue for hydrological impacts. Previous studies of rainfall in space-time suggest consistent results are expected, but this would need to be confirmed.

~~Practitioners are typically used to work with IDF curves and how they evolve with climate change. In order to further link the results obtained in this paper with previous findings, often expressed in terms of return periods, it would be needed to continue exploring the theoretical links between UM parameters and IDF curves. This is a topic currently under investigation, relying on initial elements to be further developed from Bendjoudi et al. (1997) or Langousis et al. (2009). Once this is achieved, the trends in UM parameters could be simply input in~~ With regard to potential impact of the work on the study of climate change, as for the other paper mentioned, the ~~theoretical shape of IDF curves and results quantitatively compared with existing work. This corresponds to stimulating work to be carried out~~underlying idea is to first establish, when possible, a relationship between rainfall extremes and surface air temperature relying on data, and then to use temperature as a proxy to predict future rainfall extremes. Such reasoning relies on a strong assumption of stationarity in the physical processes generating rainfall, which may not be valid. This issue was not addressed in this work which focused on exploring the link between rainfall variability and extremes with temperature relying on current data, and should be investigated in future work.

Code and data availability. Data used in the paper, i.e. the rainfall and temperature time series with 30 s time steps for the three measurement campaigns, along with a python script containing the functions needed to implement the spectral and multifractal analysis carried out in this paper can be found in Gires (2025).

6 ~~Appendix A~~

~~Number of studied samples in individual sample analysis at large scales. Campaign name # of samples in total # of events after criteria on T # events after criteria on~~ ~~r^2~~ ~~and~~ ~~$< T >$~~ ~~ENPC Campus 197 172 131 SIRTA 27 22 19 Pays d'Othe 84 63 63~~

~~Number of studied event in individual event analysis at event scale. Campaign name # of events in total # of events after removing too short ones or missing~~ $\cancel{T}$ ~~# events after criteria on~~ $\cancel{r^2}$ ~~and~~ $\cancel{<T>}$ ~~ENPC Campus 785 (2071) 644 583 SIRTA 113 (207) 84 74 Pays d'Othe 389 (1043) 316 288~~

~~Number of studied samples in ensemble analysis of samples binned according to average temperature. Bins of~~ $\cancel{2^oC}$ ~~width are used and the middle of the bin is reported in the table Temperature 3 5 7 9 11 13 15 17 19 21 23 # samples in large scale 1 4 15 22 16 20 15 20 16 22 14 # samples in large scale 48 91 144 218 223 147 119 143 103 36 15~~

Author contributions. A.G. designed the initial content of the study. Y.T. implemented the initial version of the study on RW-Turb campaign under supervision of A.G.. A.G. extended it to the other campaigns and wrote the paper. Y.T. reviewed the paper.

Competing interests. The authors declare that they have no competing interests

Acknowledgements. The authors acknowledge partial financial support from the Chair of Hydrology for Resilient Cities (endowed by Veolia) of the École nationale des ponts et chaussées, EU NEW INTERREG IV RainGain Project, EU Climate KIC Blue Green Dream project, the Île-de-France region RadX@IdF Project, and the ANR JCJC RW-Turb project (ANR-19-CE05-0022-01); which enabled the collection of data. Authors acknowledge the France-Taiwan Ra2DW project, supported by the French National Research Agency (ANR-23-CE01-0019-01) for partial financial support.

References

References

Bendjoudi, H., Hubert, P., Schertzer, D., and Lovejoy, S.: Interprétation multifractale des courbes intensité-durée-fréquence des précipitations, Comptes Rendus de l'Académie des Sciences - Series IIA - Earth and Planetary Science, 325, 323–326, https://doi.org/10.1016/S1251-8050(97)81379-1, 1997.

Borga, M., Stoffel, M., Marchi, L., Marra, F., and Jakob, M.: Hydrogeomorphic response to extreme rainfall in headwater systems: Flash floods and debris flows, Journal of Hydrology, 518, 194–205, https://doi.org/10.1016/j.jhydrol.2014.05.022, 2014.

Capozzi, V., Annella, C., Montopoli, M., Adirosi, E., Fusco, G., and Budillon, G.: Influence of Wind-Induced Effects on Laser Disdrometer Measurements: Analysis and Compensation Strategies, Remote Sensing, 13, https://doi.org/10.3390/rs13153028, 2021.

Chagnaud, G., Blanchet, J., Evin, G., Hingray, B., Lebel, T., Panthou, G., and Vischel, T.: How fast is the frequency of precipitation extremes doubling in global land regions?, Environmental Research Communications, 6, 121 010, https://doi.org/10.1088/2515-7620/ad9f12, 2024.

Chen, Y., Li, W., Jiang, X., Zhai, P., and Luo, Y.: Detectable Intensification of Hourly and Daily Scale Precipitation Extremes across Eastern China, Journal of Climate, 34, 1185 – 1201, https://doi.org/10.1175/JCLI-D-20-0462.1, 2021.

Chinchella, E., Cauteruccio, A., and Lanza, L. G.: Quantifying the Wind-Induced Bias of Rainfall Measurements for the Thies CLIMA Optical Disdrometer, Water Resources Research, 60, https://doi.org/10.1029/2024WR037366, 2024.

Dallan, E., Borga, M., Fosser, G., Canale, A., Roghani, B., Marani, M., and Marra, F.: A Method to Assess and Explain Changes in Sub-Daily Precipitation Return Levels From Convection-Permitting Simulations, Water Resources Research, 60, https://doi.org/10.1029/2023WR035969, 2024.

de Lima, M. and Grasman, J.: Multifractal analysis of 15-min and daily rainfall from a semi-arid region in Portugal, Journal of Hydrology, 220, 1–11, https://doi.org/10.1016/S0022-1694(99)00053-0, 1999.

de Montera, L., Barthès, L., Mallet, C., and Golé, P.: The Effect of Rain–No Rain Intermittency on the Estimation of the Universal Multifractals Model Parameters, Journal of Hydrometeorology, 10, 493 – 506, https://doi.org/10.1175/2008JHM1040.1, 2009.

Douglas, E. M. and Barros, A. P.: Probable Maximum Precipitation Estimation Using Multifractals: Application in the Eastern United States, Journal of Hydrometeorology, 4, 1012 – 1024, https://doi.org/10.1175/1525-7541(2003)004<1012:PMPEUM>2.0.CO;2, 2003.

Drobinski, P., Alonzo, B., Bastin, S., Silva, N. D., and Muller, C.: Scaling of precipitation extremes with temperature in the French Mediterranean region: What explains the hook shape?, Journal of Geophysical Research: Atmospheres, 121, 3100–3119, https://doi.org/10.1002/2015JD023497, 2016.

Fowler, H. J., Lenderink, G., Prein, A. F., Westra, S., Allan, R. P., Ban, N., Barbero, R., Berg, P., Blenkinsop, S., Do, H. X., Guerreiro, S., Haerter, J. O., Kendon, E. J., Lewis, E., Schaer, C., Sharma, A., Villarini, G., Wasko, C., and Zhang, X.: Anthropogenic intensification of short-duration rainfall extremes, Nature Reviews Earth & Environment, 2, 107–122, https://doi.org/10.1038/s43017-020-00128-6, 2021.

Gires, A.: Data for "A Universal Multifractals perspective into the link between rainfall extremes and temperature", https://doi.org/10.5281/zenodo.16406221, 2025.

Gires, A., Tchiguirinskaia, I., Schertzer, D., and Lovejoy, S.: Influence of the zero-rainfall on the assessment of the multifractal parameters, Advances in Water Resources, 45, 13–25, http://www.sciencedirect.com/science/article/pii/S0309170812000814, 2012.

Gires, A., Tchiguirinskaia, I., and Schertzer, D.: Multifractal comparison of the outputs of two optical disdrometers, Hydrological Sciences Journal, 61, 1641–1651, https://doi.org/10.1080/02626667.2015.1055270, 2016.

Gires, A., Tchiguirinskaia, I., and Schertzer, D.: Two months of disdrometer data in the Paris area, Earth System Science Data, 10, 941–950, https://doi.org/10.5194/essd-10-941-2018, 2018.

Gires, A., Jose, J., Tchiguirinskaia, I., and Schertzer, D.: Three months of combined high resolution rainfall and wind data collected on a wind farm, Earth System Science Data Discussions, 2022, 1–19, https://doi.org/10.5194/essd-2021-463, 2022.

Haerter, J. O. and Berg, P.: Unexpected rise in extreme precipitation caused by a shift in rain type?, Nature Geoscience, 2, 372–373, https://doi.org/10.1038/ngeo523, 2009.

Haerter, J. O., Berg, P., and Hagemann, S.: Heavy rain intensity distributions on varying time scales and at different temperatures, Journal of Geophysical Research: Atmospheres, 115, https://doi.org/10.1029/2009JD013384, 2010.

Jose, J., Gires, A., Roustan, Y., Schnorenberger, E., Tchiguirinskaia, I., and Schertzer, D.: Multifractal analysis of wind turbine power and rainfall from an operational wind farm – Part 1: Wind turbine power and the associated biases, Nonlinear Processes in Geophysics, 31, 587–602, https://doi.org/10.5194/npg-31-587-2024, 2024a.

Jose, J., Gires, A., Schnorenberger, E., Roustan, Y., Schertzer, D., and Tchiguirinskaia, I.: Multifractal analysis of wind turbine power and rainfall from an operational wind farm – Part 2: Joint analysis of available wind power and rain intensity, Nonlinear Processes in Geophysics, 31, 603–624, https://doi.org/10.5194/npg-31-603-2024, 2024b.

Ladoy, P., Schmitt, F., Schertzer, D., and Lovejoy, S.: The multifractal temporal variability of nimes rainfall data, Comptes Rendus de l'Academie Des Sciences Serie Ii, 317, 775–782, 1993.

Langousis, A., Veneziano, D., Furcolo, P., and Lepore, C.: Multifractal rainfall extremes: Theoretical analysis and practical estimation, Chaos, Solitons Fractals, 39, 1182–1194, https://doi.org/https://doi.org/10.1016/j.chaos.2007.06.004, 2009.

Lanza, L. G., Merlone, A., Cauteruccio, A., Chinchella, E., Stagnaro, M., Dobre, M., Garcia Izquierdo, M. C., Nielsen, J., Kjeldsen, H., Roulet, Y. A., Coppa, G., Musacchio, C., Bordianu, C., and Parrondo, M.: Calibration of non-catching precipitation measurement instruments: A review, Meteorological Applications, 28, e2002, https://doi.org/https://doi.org/10.1002/met.2002, 2021.

Lavallée, D., Lovejoy, S., and Ladoy, P.: Nonlinear variability and landscape topography: analysis and simulation, in: Fractas in geography, edited by de Cola, L. and Lam, N., pp. 171–205, Prentice-Hall, 1993.

Lenderink, G. and van Meijgaard, E.: Increase in hourly precipitation extremes beyond expectations from temperature changes, Nature Geoscience, 1, 511–514, https://doi.org/10.1038/ngeo262, 2008.

Lenderink, G., Barbero, R., Loriaux, J. M., and Fowler, H. J.: Super-Clausius–Clapeyron Scaling of Extreme Hourly Convective Precipitation and Its Relation to Large-Scale Atmospheric Conditions, Journal of Climate, 30, 6037 – 6052, https://doi.org/10.1175/JCLI-D-16-0808.1, 2017.

Li, C., Zwiers, F., Zhang, X., Chen, G., Lu, J., Li, G., Norris, J., Tan, Y., Sun, Y., and Liu, M.: Larger Increases in More Extreme Local Precipitation Events as Climate Warms, Geophysical Research Letters, 46, 6885–6891, https://doi.org/10.1029/2019GL082908, 2019.

Lovejoy, S. and Schertzer, D.: Comment on "Are rain rate processes self-similar?" by B. Kedem and L. S. Chiu, Water Resources Research, 25, 577–579, https://doi.org/10.1029/WR025i003p00577, 1989.

Lovejoy, S. and Schertzer, D.: Multifractals and rain, in: New Uncertainty Concepts in Hydrology and Hydrological modelling, edited by Kundzewicz, A. W., pp. 62–103, Cambridge Press, 1995.

Lovejoy, S. and Schertzer, D.: Scaling and multifractal fields in the solid earth and topography, Nonlinear Processes in Geophysics, 14, 465–502, https://doi.org/10.5194/npg-14-465-2007, 2007.

Mandapaka, P. V., Lewandowski, P., Eichinger, W. E., and Krajewski, W. F.: Multiscaling analysis of high resolution space-time lidar-rainfall, Nonlinear Processes in Geophysics, 16, 579–586, https://doi.org/10.5194/npg-16-579-2009, 2009.

Marra, F., Koukoula, M., Canale, A., and Peleg, N.: Predicting extreme sub-hourly precipitation intensification based on temperature shifts, Hydrology and Earth System Sciences, 28, 375–389, https://doi.org/10.5194/hess-28-375-2024, 2024.

Masson-Delmotte, V., Zhai, P., Pirani, A., Connors, S., Péan, C., Caud, S. B. N., Chen, Y., Goldfarb, L., Gomis, M., Huang, M., Leitzell, K., Lonnoy, E., Matthews, J., Maycock, T., Waterfield, T., Yelekçi, O., Yu, R., and Zhou, B.: IPCC, 2021: Climate Change 2021: The Physical Science Basis. Contribution of Working Group I to the Sixth Assessment Report of the Intergovernmental Panel on Climate Change, 2021.

Moustakis, Y., Onof, C. J., and Paschalis, A.: Atmospheric convection, dynamics and topography shape the scaling pattern of hourly rainfall extremes with temperature globally, Communications Earth & Environment, 1, 11, https://doi.org/10.1038/s43247-020-0003-0, 2020.

Moustakis, Y., Papalexiou, S. M., Onof, C. J., and Paschalis, A.: Seasonality, Intensity, and Duration of Rainfall Extremes Change in a Warmer Climate, Earth's Future, 9, e2020EF001 824, https://doi.org/10.1029/2020EF001824, 2021.

O'Gorman, P. A.: Precipitation Extremes Under Climate Change, Current Climate Change Reports, 1, 49–59, https://doi.org/10.1007/s40641-015-0009-3, 2015.

Panthou, G., Mailhot, A., Laurence, E., and Talbot, G.: Relationship between Surface Temperature and Extreme Rainfalls: A Multi-Time-Scale and Event-Based Analysis, Journal of Hydrometeorology, 15, 1999 – 2011, https://doi.org/10.1175/JHM-D-14-0020.1, 2014.

Parisi, G. and Frisch, U.: A multifractal model of intermittency, in: Turbulence and predictability in geophysical fluid dynamics, edited by Ghill, M., Benzi, R., and Parisi, G., pp. 111–114, Elsevier North Holland, New-York, 1985.

Peleg, N., Marra, F., Fatichi, S., Molnar, P., Morin, E., Sharma, A., and Burlando, P.: Intensification of Convective Rain Cells at Warmer Temperatures Observed from High-Resolution Weather Radar Data, Journal of Hydrometeorology, 19, 715 – 726, https://doi.org/10.1175/JHM-D-17-0158.1, 2018.

Qiu, Y., Schertzer, D., Tisserand, B., and Tchiguirinskaia, I.: Spatio-temporal rainfall variability and its impacts on the hydrological response of nature-based solutions, Urban Water Journal, 21, 1147–1163, https://doi.org/10.1080/1573062X.2023.2180395, 2024.

Royer, J.-F., Biaou, A., Chauvin, F., Schertzer, D., and Lovejoy, S.: Multifractal analysis of the evolution of simulated precipitation over France in a climate scenario, C.R Geoscience, 340, 431–440, 2008.

Schertzer, D. and Lovejoy, S.: Physical modeling and analysis of rain and clouds by anisotropic scaling multiplicative processes, Journal of Geophysical Research: Atmospheres, 92, 9693–9714, https://doi.org/https://doi.org/10.1029/JD092iD08p09693, 1987.

Schertzer, D. and Lovejoy, S.: Universal Multifractals Do Exist!: Comments on "A Statistical Analysis of Mesoscale Rainfall as a Random Cascade", Journal of Applied Meteorology, 36, 1296 – 1303, https://doi.org/10.1175/1520-0450(1997)036<1296:UMDECO>2.0.CO;2, 1997.

Schertzer, D. and Tchiguirinskaia, I.: A Century of Turbulent Cascades and the Emergence of Multifractal Operators, Earth and Space Science, 7, e2019EA000 608, https://doi.org/10.1029/2019EA000608, 2020.

Schleiss, M.: How intermittency affects the rate at which rainfall extremes respond to changes in temperature, Earth System Dynamics, 9, 955–968, https://doi.org/10.5194/esd-9-955-2018, 2018.

Sharma, S. and Mujumdar, P.: On the relationship of daily rainfall extremes and local mean temperature, Journal of Hydrology, 572, 179–191, https://doi.org/10.1016/j.jhydrol.2019.02.048, 2019.

Tessier, Y., Lovejoy, S., and Schertzer, D.: Universal Multifractals: Theory and Observations for Rain and Clouds, Journal of Applied Meteorology and Climatology, 32, 223 – 250, https://doi.org/10.1175/1520-0450(1993)032<0223:UMTAOF>2.0.CO;2, 1993.

Verrier, S., de Montera, L., Barthès, L., and Mallet, C.: Multifractal analysis of African monsoon rain fields, taking into account the zero rain-rate problem, Journal of Hydrology, 389, 111–120, https://doi.org/10.1016/j.jhydrol.2010.05.035, 2010.